AN APPLICATION OF THE CAGNIARD-DE HOOP TECHNIQUE FOR SOLVING INITIAL-BOUNDARY VALUE PROBLEMS IN BOUNDED REGIONS

by M. ŠTUMPF[†,*]

(*Electrical Engineering Department, ESAT-TELEMIC, Katholieke Universiteit Leuven, Kasteelpark Arenberg 10, Heverlee (Leuven)* B-3001*, Belgium*)

[Received 17 April 2012. Revise 6 December 2012. Accepted 19 December 2012]

Dedicated to Professor A. T. De HOOP, (*Lorentz Chair Emeritus Professor, Laboratory of Electromagnetic Research, Delft University of Technology, Mekelweg 4, 2628 CD Delft, the Netherlands*)

Summary

An application of the Cagniard–De Hoop method for solving a class of initial-boundary value problems in bounded regions is presented. A procedure is briefly formulated and subsequently applied to acoustic and electromagnetic wave propagation problems in layered media. A simple example with illustrative numerical results is given.

1. Introduction

The Cagniard–De Hoop technique is a sophisticated mathematical tool for solving a collection of wave and diffusive problems in various branches of physics. The method has been originally developed for tackling transient seismic problems (**1**–**6**) and has found wealth of applications in electromagnetics (**7**–**11**), acoustics (**12**), (**13**) and elastodynamics (**14**–**16**). The Cagniard–De Hoop technique has proved to be a useful tool that yields closed-form expressions for problems with an impulsive source in a discretely layered medium (**17**) as well as in a continuously layered medium (**18**), (**19**). The latter has been originally analysed by Chapman using the Pekeris modification of the Cagniard technique (**20**). The main ingredient of the Cagniard–De Hoop method is a unilateral Laplace transformation with respect to time with a positive and real transform parameter which is subsequently used as a scaling parameter in a Fourier representation parallel to a stratification. An application of the integral transformations requires the time invariance and the shift (spatial) invariance along the layering of the problem configuration. As a consequence of the latter, a direct application of the Cagniard–De Hoop method to initial-boundary value problems defined over bounded regions is not possible.

A class of problems discussed in this article is almost exclusively solved with the aid of the separation of variables technique with subsequent solution of corresponding eigenvalue problems via eigenfunction (or modal) expansions in space and time (**21**, Section 4.2). In such series expansions all time-domain constituents for a given field point arise at the same time that does not depend on the spatial coordinate along which the modal expansion applies. An example of this property is the

[†]martin.stumpf@centrum.cz

[*]On leave from Brno University of Technology, SIX Research Centre, Purkyňova 118, 612 00 Brno, the Czech Republic.

Q. Jl Mech. Appl. Math, Vol. 66. No. 2 © The Author, 2013. Published by Oxford University Press; all rights reserved. For Permissions, please email: journals.permissions@oup.com
Advance Access publication 15 February 2013. doi:10.1093/qjmam/hbs025

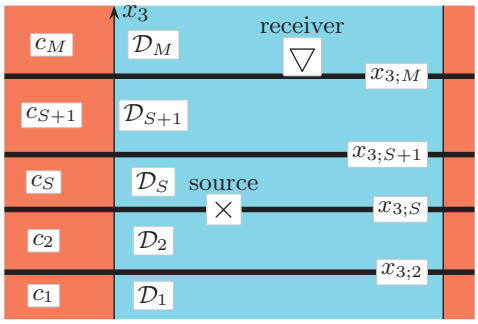

Fig. 1 Horizontally stratified and laterally bounded medium in which wavefields are generated by an impulsive source (Colour version of the figure is available online at *QJMAM*)

'axial arrival time' in a modal solution for cylindrical waveguide structures (see (**22**, Equation (15))) or absence of the arrival time in modal expansions connected with completely closed 'resonator' problems. An important feature of the modal-expansion solution is an oscillating behaviour of modal constituents that gradually increases with the growing order of eigenvalues. This property can make numerical evaluation of the time convolution with a source signature delicate, especially for high-order constituents. The nature of the modal solution thus limits its applications for late-time responses, for field points far away from an activating source.

Fortunately, still another series expansions does exist that can circumvent all mentioned difficulties. It can be found more or less intuitively or from the modal-expansion solution upon application of Poisson's summation formula (**23**, Section B.4). Such solution has a clear interpretation as a set of contributions from 'image sources' and is therefore called as the image-source expansion (**24**, Section 7.2). The image-source approach preserves a property that the time-domain constituents that arise from successive reflections against pertaining boundaries arrive to the field point at a later time than the previous ones. It is therefore suitable for a combination with the Cagniard–De Hoop technique, which is exactly the objective of this article.

2. Problem formulation

A generic problem under consideration is given in Fig. 1. The position in the problem configuration is localized by the coordinates $\{x_1, x_2, x_3\}$ with respect to a fixed, orthogonal, right-handed Cartesian reference frame. The spatial reference frame is defined with respect to the origin O and the three mutually perpendicular base vectors $\{\boldsymbol{i}_1, \boldsymbol{i}_2, \boldsymbol{i}_3\}$ of unit length each; they form, in the indicated order, a right-handed system. The subscript notation for Cartesian tensors with the summation convention for repeated subscripts is employed. The Levi-Civita tensor (completely antisymmetrical tensor of rank 3) is $\boldsymbol{e}_{k,m,p} = 1$ for $\{k, m, p\} =$ even permutation of $\{1, 2, 3\}$, $\boldsymbol{e}_{k,m,p} = -1$ for $\{k, m, p\} =$ odd permutation of $\{1, 2, 3\}$ and $\boldsymbol{e}_{k,m,p} = 0$ in all other cases. Lower-case Latin subscripts stand for the values $\{1, 2, 3\}$ whereas lower-case Greek subscripts stand for the values $\{1, 2\}$. Within the reference frame, the position of a point is defined by the position vector $\boldsymbol{x} = x_k \boldsymbol{i}_k$. The spatial differentiation with respect to x_m is denoted by ∂_m. The time coordinate is denoted by t and symbol ∂_t is reserved for the partial differentiation with respect to time.

The configuration consists of a time-invariant stratified medium which properties vary in vertical direction and which is laterally bounded by impenetrable plane boundaries. The layered medium consists of M domains $\mathcal{D}_N = \{0 < x_1 < W_1, 0 < x_2 < W_2, x_{3;N} < x_3 < x_{3;N+1}\}$ where $\mathcal{D} = \cup_{N=1}^{M} \mathcal{D}_N$. Each of domains $\mathcal{D}_N$ is characterized by the corresponding wavespeed c_N for $N = \{1, ..., M\}$ and by its lengths of sides $d_N = x_{3;N+1} - x_{3;N}$ for $N = \{2, ..., M-1\}$ and $W_1 > 0$, $W_2 > 0$. The wavefield is radiated by an impulsive source that is located at $\boldsymbol{x} = \boldsymbol{x}_S$. The source level $x_3 = x_{3;S}$ is placed at the interface of two domains with non-zero or zero contrast in their properties. The latter can be considered as the source placed within one domain. Consequently, the response is probed at the receiving point that can be defined either at the interface or within a domain. It is assumed that a source starts to act at $t = 0$ and that prior to this instant the wavefields vanish throughout the configuration.

Let consider the scalar wave u generated by an impulsive point source that satisfies the three-dimensional wave equation,

$$\partial_k \partial_k u - c^{-2} \partial_t^2 u = -\delta(\boldsymbol{x} - \boldsymbol{x}_S) F(t), \tag{2.1}$$

in $\mathcal{D}$ for $t > 0$. Here, $\delta(\boldsymbol{x})$ is the three-dimensional Dirac distribution. For the source signature $F(t)$ we assume $F(t) = 0$ for $t < 0$ and also for the wave function $u(\boldsymbol{x}, t) = 0$ and $\partial_t u(\boldsymbol{x}, t) = 0$ for $t < 0$. The wavespeed is assumed to be a piecewise constant function along the vertical direction $c = c(x_3)$. Across each source-free interface where the wavespeed shows a jump discontinuity we assume that u and $\partial_3 u$ are continuous,

$$\lim_{x_3 \downarrow x_{3;N}} \{u, \partial_3 u\}(\boldsymbol{x}, t) = \lim_{x_3 \uparrow x_{3;N}} \{u, \partial_3 u\}(\boldsymbol{x}, t), \tag{2.2}$$

for $\{0 < x_1 < W_1, 0 < x_2 < W_2\}$ and for all $t > 0$. In the case of an impenetrable horizontal boundary we assume

$$\lim_{x_3 \uparrow x_{3;M}} u(\boldsymbol{x}, t) = 0 \quad \text{or} \quad \lim_{x_3 \uparrow x_{3;M}} \partial_3 u(\boldsymbol{x}, t) = 0 \tag{2.3}$$

or/and

$$\lim_{x_3 \downarrow x_{3;2}} u(\boldsymbol{x}, t) = 0 \quad \text{or} \quad \lim_{x_3 \downarrow x_{3;2}} \partial_3 u(\boldsymbol{x}, t) = 0, \tag{2.4}$$

for $\{0 < x_1 < W_1, 0 < x_2 < W_2\}$ and for all $t > 0$. The normal derivative of the wave function across the source level gives the excitation condition

$$\lim_{x_3 \downarrow x_{3;S}} \partial_3 u(\boldsymbol{x}, t) - \lim_{x_3 \uparrow x_{3;S}} \partial_3 u(\boldsymbol{x}, t) = -\delta(x_1 - x_{1;S}) \delta(x_2 - x_{2;S}) F(t), \tag{2.5}$$

for $\{0 < x_1 < W_1, 0 < x_2 < W_2\}$ and for all $t > 0$. Here $\delta(x)$ denotes the one-dimensional Dirac distribution. Along the vertical plane boundaries the wave function satisfies

$$\lim_{x_\mu \downarrow 0} u(\boldsymbol{x}, t) = 0 \quad \text{or} \quad \lim_{x_\mu \downarrow 0} \partial_\mu u(\boldsymbol{x}, t) = 0 \tag{2.6}$$

or/and

$$\lim_{x_\mu \uparrow W_\mu} u(\boldsymbol{x}, t) = 0 \quad \text{or} \quad \lim_{x_\mu \uparrow W_\mu} \partial_\mu u(\boldsymbol{x}, t) = 0, \tag{2.7}$$

for all $t > 0$ and $x_3 \in \mathbb{R}$.

3. Problem solution

The problem formulated in the previous section is not shift invariant along the direction parallel to the stratification and as a consequence the Cagniard–De Hoop cannot be applied directly. Instead of applying discrete Fourier expansions along the layering we express the solution in the form

$$u(\boldsymbol{x}, t) = u^F(\boldsymbol{x}, t) + u^G(\boldsymbol{x}, t), \tag{3.1}$$

where u^F is the fundamental solution that satisfies the three-dimensional wave equation (2.1) with the boundary conditions along the horizontal interfaces (2.2)–(2.5) extended over $\{-\infty < x_1 < \infty, -\infty < x_2 < \infty\}$. The fundamental solution does not satisfy the boundary condition along the vertical planes and can be found via the Cagniard–De Hoop method. The second part of the solution u^G satisfies the same boundary conditions along horizontal boundaries and is adjusted such that the boundary conditions along the vertical boundaries (2.6) and (2.7) are satisfied. The solution u^G is not singular in $\mathcal{D}$ and obeys here the homogeneous three-dimensional wave equation

$$\partial_k \partial_k u^G - c^{-2} \partial_t^2 u^G = 0, \tag{3.2}$$

for $t > 0$. The scalar wave function u^G can be interpreted as to be generated by 'image sources'. The fundamental solution follows from (2.1)–(2.5) upon application of a unilateral Laplace transformation with respect to time with the real-valued and positive parameter s relying on Lerch's uniqueness theorem (**25**, Section 5) in combination with the wave slowness field representation along the problem stratification. This leads to the transform-domain field equations that are solved in an iterative manner via the generalized-ray expansion and subsequently transformed back to space-time (**17**). The auxiliary solution u^G and subsequently the total solution u can be then constructed based on the symmetry properties of the fundamental solution u^F. Without loss of generality let us analyse the plane boundaries $x_1 = \{0, W_1\}$ only. Since the fundamental solution satisfies

$$u^F(x_1, x_2, x_3, t) = u^F(-x_1, x_2, x_3, t) \tag{3.3}$$

$$\partial_1 u^F(x_1, x_2, x_3, t) = -\partial_1 u^F(-x_1, x_2, x_3, t), \tag{3.4}$$

we can write the total solution as

$$\begin{aligned} u(x_1, x_2, x_3, t) = &\sum_{m=-\infty}^{\infty} (\pm 1)^m u^F(x_1 | x_{1;S} + 2mW_1, x_2, x_3, t) \\ &\pm \sum_{m=-\infty}^{\infty} (\pm 1)^m u^F(x_1 | 2mW_1 - x_{1;S}, x_2, x_3, t), \end{aligned} \tag{3.5}$$

for $\partial_1 u = 0$ or $u = 0$ along the vertical planes $x_1 = \{0, W_1\}$. Here $x_{1;S} + 2mW_1$ and $2mW_1 - x_{1;S}$ are the positions of sources along x_1 axis. The procedure for the plane boundaries along $x_2 = \{0, W_2\}$ goes along the same lines. Note that the arrival times of contributions from the image sources increase together with $|m|$. This has the consequence that the time-domain constituent arises at a later time then the previous one. Based on the fact that one is always interested in the wave field in a finite time window of observation, a finite number of time-domain constituents in the image-source expansion (3.5) is in practice sufficient to get the exact time-domain response. The image-source expansions can be interpreted as the sets of (generalised-)rays reflecting against corresponding boundaries.

4. Construction of the fundamental solution

To construct the fundamental solution we subject wavefield quantities to a unilateral Laplace transformation:

$$\hat{u}^F(\boldsymbol{x}, s) = \int_{t=0}^{\infty} \exp(-st) u^F(\boldsymbol{x}, t) dt, \tag{4.1}$$

where the transform parameter s is taken to be real-valued and positive relying on Lerch's uniqueness theorem (**25**, Section 5). In view of the shift invariance along a direction parallel to the layering we in addition apply the wave slowness field representation:

$$\begin{aligned}\hat{u}^F(x_1, x_2, x_3, s) = (s/2\pi)^2 \int_{\alpha_1=-\infty}^{\infty} d\alpha_1 \\ \times \int_{\alpha_2=-\infty}^{\infty} \exp[-\mathrm{i}\, s(\alpha_1 x_1 + \alpha_2 x_2)] \tilde{u}^F(\alpha_1, \alpha_2, x_3, s) d\alpha_2,\end{aligned} \tag{4.2}$$

which implies $\tilde{\partial}_\mu = -\mathrm{i}s\alpha_\mu$, $\alpha_\mu \in \mathbb{R}$. In each subdomain $\mathcal{D}_N$ of the configuration, the transform-domain (bounded) solution can be written

$$\tilde{u}_N^F = W_N^+ \exp[-s\gamma_N(x_3 - x_{3;N})] + W_N^- \exp[-s\gamma_N(x_{3;N+1} - x_3)], \tag{4.3}$$

where $\{W_N^+, W_N^-\}$ are upogoing/downgoing transform-domain wave amplitudes and the vertical propagation factor is

$$\gamma_N(\alpha_1, \alpha_2) = \left(c_N^{-2} + \alpha_1^2 + \alpha_2^2\right)^{1/2} \tag{4.4}$$

with $\mathrm{Re}(\gamma_N) \geqslant 0$ for all $p \in \mathbb{C}$. The transform-domain wave amplitudes are mutually related at each interface via the scattering-matrix description (**17**):

$$W_N^+ = \bar{S}_N^{+-} W_N^- + \bar{S}_N^{++} W_{N-1}^+ + X_N^+ \tag{4.5}$$

$$W_{N-1}^- = \bar{S}_N^{--} W_N^- + \bar{S}_N^{-+} W_{N-1}^+ + X_{N-1}^-, \tag{4.6}$$

for $N = \{2, ..., M\}$ with $W_1^+ = W_M^- = 0$. Here, $S_N^{\pm\pm}$ and $\{X_N^+, X_{N-1}^-\}$ are scattering and source-coupling parameters, respectively. For horizontally stratified medium consisting of M domains and $M-1$ interfaces we arrive at the $(2M-2) \times (2M-2)$ scattering matrix $\bar{\boldsymbol{S}}$ with $4(M-2)$ scattering parameters. Symbolically, the transform-domain constituents are finally iteratively generated in the following way:

$$\boldsymbol{W} = \sum_{r=0}^{R} \bar{\boldsymbol{S}}^r \cdot \boldsymbol{X} + \bar{\boldsymbol{S}}^{R+1} \cdot \boldsymbol{W}. \tag{4.7}$$

Here, $\boldsymbol{W}$ is the vector of transform-domain wave amplitudes and $\boldsymbol{X}$ is the source-coupling vector. Once the scattering and source-coupling parameters are known, (4.7) can be transformed back to

space-time using the Cagniard–De Hoop inversion procedure. A space-time counterpart of each term in the sum of (4.7) is denoted as a generalised-ray constituent. Since its arrival time increases with r, all terms from a certain value R onward can be ignored. Examples of full-vectorial solutions for acoustic and electromagnetic waves in layered media are constructed in the next subsections. In them we take $F(t) = \delta(t)$.

4.1 *Acoustic waves in a layered fluid*

Acoustic properties of each subdomain $\mathcal{D}_N$ are described by its volume density of mass ρ_N and compressibility κ_N with $c_N = (\rho_N \kappa_N)^{-1/2}$. In the following example we consider an acoustic monopole source defined by its volume source density of injection rate,

$$q(\boldsymbol{x}, t) = Q(t)\delta(x_1, x_2, x_3 - x_{3;S}), \tag{4.8}$$

and by vanishing volume source density of force $f_k = 0$. Here, $Q(t)$ is the source signature. The transform-domain solution for the acoustic pressure and the vertical component of the particle velocity can be then constructed as

$$\tilde{p}^F_N(\alpha_1, \alpha_2, x_3, s) = s\rho_N \hat{Q}(s)\tilde{u}^F_N(\alpha_1, \alpha_2, x_3, s) \tag{4.9}$$

$$\tilde{v}^F_{3;N}(\alpha_1, \alpha_2, x_3, s) = -\hat{Q}(s)\partial_3 \tilde{u}^F_N(\alpha_1, \alpha_2, x_3, s) \tag{4.10}$$

with the in-plane components of the particle velocity expressed via

$$\tilde{v}^F_{\kappa;N}(\alpha_1, \alpha_2, x_3, s) = -\tilde{\partial}_\kappa \tilde{p}^F_N(\alpha_1, \alpha_2, x_3, s)/s\rho_N. \tag{4.11}$$

Continuity of the acoustic pressure and the vertical component of the particle velocity across the interfaces (see (2.2)) implies the scattering parameters corresponding to the N-th interface:

$$S^{+-}_N = (\gamma_N/\rho_N - \gamma_{N-1}/\rho_{N-1})/(\gamma_N/\rho_N + \gamma_{N-1}/\rho_{N-1}) \tag{4.12}$$

$$S^{-+}_N = (\gamma_{N-1}/\rho_{N-1} - \gamma_N/\rho_N)/(\gamma_{N-1}/\rho_{N-1} + \gamma_N/\rho_N) \tag{4.13}$$

$$S^{--}_N = (2\gamma_N/\rho_{N-1})/(\gamma_N/\rho_N + \gamma_{N-1}/\rho_{N-1}) \tag{4.14}$$

$$S^{++}_N = (2\gamma_{N-1}/\rho_N)/(\gamma_{N-1}/\rho_{N-1} + \gamma_N/\rho_N). \tag{4.15}$$

If the fluid is confined between impenetrable boundaries from above or/and below (see (2.3) and (2.4)) then the corresponding scattering parameters are given as

$$S^{+-}_2 = \pm 1 \quad \text{or/and} \quad S^{-+}_M = \pm 1, \tag{4.16}$$

along a perfectly rigid boundary (+) and along a pressure-release boundary (−), respectively. The corresponding source-coupling coefficients differ from zero only at the source level:

$$X^-_{S-1} = 1/[s\rho_{S-1}(\gamma_S/\rho_S + \gamma_{S-1}/\rho_{S-1})] \tag{4.17}$$

$$X^+_S = 1/[s\rho_S(\gamma_S/\rho_S + \gamma_{S-1}/\rho_{S-1})], \tag{4.18}$$

which follow from the excitation condition (see (2.5)). In this respect, a two-dimensional acoustic problem for $M = 2$ (fluid half-spaces) is solved in (**26**) via the Cagniard–De Hoop method with the time Fourier transform.

4.2 *Electromagnetic waves in layered media*

Electromagnetic properties of each subdomain $\mathcal{D}_N$ are described by its electric permittivity ϵ_N and magnetic permeability μ_N with $c_N = (\epsilon_N \mu_N)^{-1/2}$. In the following example we consider a vertical electric dipole source defined by its electric current volume density:

$$J_3(\boldsymbol{x}, t) = J(t)\delta(x_1, x_2, x_3 - x_{3;S}), \tag{4.19}$$

where $J(t)$ is the source signature. The transform-domain solution for the electric and magnetic field strengths $\tilde{E}_k$ and $\tilde{H}_j$, respectively, can be then constructed as

$$\tilde{E}^F_{\pi;N}(\alpha_1, \alpha_2, x_3, s) = \tilde{\partial}_\pi \partial_3 \hat{J}(s)\tilde{u}^F_N(\alpha_1, \alpha_2, x_3, s)/s\epsilon_N \tag{4.20}$$

$$\tilde{H}^F_{\rho;N}(\alpha_1, \alpha_2, x_3, s) = \boldsymbol{e}_{\rho,\pi,3}\tilde{\partial}_\pi \hat{J}(s)\tilde{u}^F_N(\alpha_1, \alpha_2, x_3, s) \tag{4.21}$$

$$\tilde{E}^F_{3;N}(\alpha_1, \alpha_2, x_3, s) = -s\mu_N \hat{J}(s)\tilde{u}^F_N(\alpha_1, \alpha_2, x_3, s) + \hat{J}(s)\partial_3^2 \tilde{u}^F_N(\alpha_1, \alpha_2, x_3, s)/s\epsilon_N. \tag{4.22}$$

Continuity of tangential components of the electric and magnetic field strength across the interfaces (see (2.2)) implies the scattering parameters corresponding to the N-th interface:

$$S^{+-}_N = (\gamma_N/\epsilon_N - \gamma_{N-1}/\epsilon_{N-1})/(\gamma_N/\epsilon_N + \gamma_{N-1}/\epsilon_{N-1}) \tag{4.23}$$

$$S^{--}_N = (2\gamma_N/\epsilon_N)/(\gamma_N/\epsilon_N + \gamma_{N-1}/\epsilon_{N-1}) \tag{4.24}$$

$$S^{-+}_N = (\gamma_{N-1}/\epsilon_{N-1} - \gamma_N/\epsilon_N)/(\gamma_{N-1}/\epsilon_{N-1} + \gamma_N/\epsilon_N) \tag{4.25}$$

$$S^{++}_N = (2\gamma_{N-1}/\epsilon_{N-1})/(\gamma_{N-1}/\epsilon_{N-1} + \gamma_N/\epsilon_N). \tag{4.26}$$

If an impenetrable interface is present (see (2.3) and (2.4)), then we can find

$$S^{+-}_2 = \pm 1 \quad \text{or/and} \quad S^{-+}_M = \pm 1 \tag{4.27}$$

along a perfect electric conductor (+) and a perfect magnetic conductor (−). The corresponding source-coupling coefficients follow again from the excitation condition (see (2.5)) as

$$X^+_S = X^-_{S-1} = 1/[s(\gamma_S/\epsilon_S + \gamma_{S-1}/\epsilon_{S-1})], \tag{4.28}$$

which completes the transform-domain solution.

5. Illustrative example

The procedure for solving initial-boundary value problems will be demonstrated on a simple example. To this end let us solve the two-dimensional scalar wave equation,

$$\left(\partial_1^2 + \partial_3^2\right) u - c^{-2}\partial_t^2 u = 0, \tag{5.1}$$

in the bounded domain $\mathcal{D} = \{0 < x_1 < W, 0 < x_3 < H\}$ (Fig. 2) together with the zero-value initial conditions $u(\boldsymbol{x}, t) = 0$ and $\partial_t u(\boldsymbol{x}, t) = 0$ for $t < 0$ and the boundary conditions along the horizontal planes:

$$\lim_{x_3 \downarrow 0} \partial_3 u = -\partial_t F(t)\delta(x_1 - x_{1;S}) \tag{5.2}$$

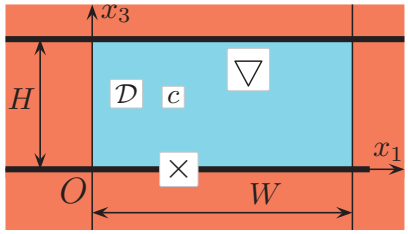

Fig. 2 Bounded two-dimensional region in which wavefield is generated by impulsive line source (Colour version of the figure is available online at *QJMAM*)

and

$$\lim_{x_3 \uparrow H} \partial_3 u = 0 \tag{5.3}$$

with $F(t) = 0$ for $t < 0$. Along the vertical boundaries we take

$$\lim_{x_1 \downarrow 0} u = 0 \quad \text{or} \quad \lim_{x_1 \downarrow 0} \partial_1 u = 0 \tag{5.4}$$

and

$$\lim_{x_1 \uparrow W} u = 0 \quad \text{or} \quad \lim_{x_1 \uparrow W} \partial_1 u = 0. \tag{5.5}$$

In the first step, the fundamental solution satisfying (5.1)–(5.3) is found via the Cagniard–De Hoop method. To this end we combine the unilateral Laplace transformation (4.1) with the wave slowness representation along x_1 axis:

$$\hat{u}^F(x_1, x_3, s) = \frac{s}{2\pi \mathrm{i}} \int_{p=-\mathrm{i}\infty}^{\mathrm{i}\infty} \exp(-spx_1) \tilde{u}^F(p, x_3, s) dp. \tag{5.6}$$

Under these transformations (5.1)–(5.3) yield the wave slowness representation of the fundamental solution,

$$\hat{u}^F(x_1, x_3, s) = \frac{s\hat{F}(s)}{2\pi \mathrm{i}} \int_{p=-\mathrm{i}\infty}^{\mathrm{i}\infty} \exp(-spX_1) \frac{\cosh[s\gamma(p)(x_3 - H)]}{\sinh[s\gamma(p)H]} \frac{dp}{\gamma(p)}, \tag{5.7}$$

with $X_1 = x_1 - x_{1;S}$ and $\gamma(p) = (1/c^2 - p^2)^{1/2}$ with $\mathrm{Re}[\gamma(p)] \geqslant 0$ for all $p \in \mathbb{C}$. Instead of evaluating the integral using the residue theorem, the integrand is expanded into the convergent geometric series and each of its terms is transformed using the Cagniard–De Hoop inversion (**1**). This procedure after a few steps leads to

$$u^F\left(x_1|x_{1;S}, x_3, t\right) = \partial_t F(t) \overset{(t)}{*} \frac{1}{\pi} \sum_{r=0}^{R} \left\{ \frac{\mathrm{H}\left[t - T_+\left(x_1|x_{1;S}, x_3\right)\right]}{\left[t^2 - T_+^2\left(x_1|x_{1;S}, x_3\right)\right]^{1/2}} + \frac{\mathrm{H}\left[t - T_-\left(x_1|x_{1;S}, x_3\right)\right]}{\left[t^2 - T_-^2\left(x_1|x_{1;S}, x_3\right)\right]^{1/2}} \right\}, \tag{5.8}$$

where $\mathrm{H}(t)$ is the Heaviside function and where

$$T_+(x_1|x_{1;S}, x_3) = \left[\left(x_1 - x_{1;S}\right)^2 + (x_3 + 2rH)^2\right]^{1/2} \tag{5.9}$$

$$T_-(x_1|x_{1;S}, x_3) = \left[\left(x_1 - x_{1;S}\right)^2 + (2rH + 2H - x_3)^2\right]^{1/2} \tag{5.10}$$

are the arrival times of the upgoing and downgoing time-domain constituents reflecting from the horizontal impenetrable boundaries. The evaluation of the integral in (5.7) using the residue theorem and its subsequent inverse Laplace transformation with the help of (**27**, 29.3.92) yields the fundamental solution in the following form:

$$u^F(x_1|x_{1;S}, x_3, t) = \frac{c}{2H}F(t - X_1/c)$$
$$+ \frac{c}{H}\partial_t F(t) \overset{(t)}{*} \sum_{m=1}^{\infty} \mathrm{J}_0\left[\frac{m\pi}{H}\left(c^2t^2 - X_1^2\right)^{1/2}\right] \mathrm{H}(t - X_1/c)\cos\left(\frac{m\pi}{H}x_3\right), \tag{5.11}$$

where $\mathrm{J}_0(x)$ is the Bessel function of the first kind and zero order. Equation (5.11) is the modal-expansion solution along the vertical direction with the axial arrival time X_1/c which will serve to demonstrate main features of modal-expansion solutions. To complete the solution of the original problem (5.1)–(5.5) we apply (3.5)–(5.8) which gives

$$u(x_1, x_3, t) = \sum_{m=-\infty}^{\infty} (\pm 1)^m u^F(x_1|x_{1;S} + 2mW_1, x_3, t)$$
$$\pm \sum_{m=-\infty}^{\infty} (\pm 1)^m u^F(x_1|2mW_1 - x_{1;S}, x_3, t), \tag{5.12}$$

for $\partial_1 u = 0$ or $u = 0$ along $x_1 = \{0, W\}$. Equation (5.12) with (5.9) and (5.10) imply that the solution of the original problem is constructed as a superposition of time-domain constituents with the arrival times:

$$T_{R+} = \left[\left(x_1 - x_{1;S} - 2mW\right)^2 + (x_3 + 2rH)^2\right]^{1/2} \tag{5.13}$$

$$T_{R-} = \left[\left(x_1 - x_{1;S} - 2mW\right)^2 + (2rH + 2H - x_3)^2\right]^{1/2} \tag{5.14}$$

$$T_{L+} = \left[\left(x_1 - 2mW + x_{1;S}\right)^2 + (x_3 + 2rH)^2\right]^{1/2} \tag{5.15}$$

$$T_{L-} = \left[\left(x_1 - 2mW + x_{1;S}\right)^2 + (2rH + 2H - x_3)^2\right]^{1/2}. \tag{5.16}$$

It is evident that the time-domain constituents successively arrive to the field point which has the consequence that only a subset of them is needed in any finite time window of observation.

6. Numerical results

This section illustrates main differences between the modal-expansion and the generalised-ray solutions. To this end the fundamental solution u^F is numerically evaluated using the expression

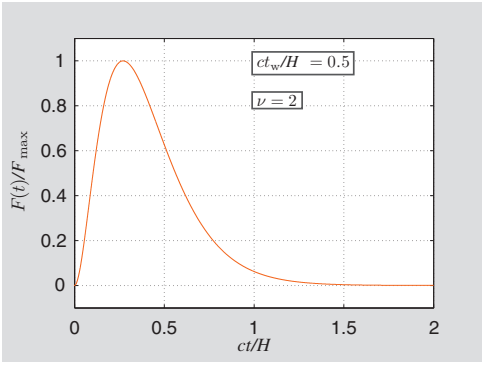

Fig. 3 Power exponential source signature (Colour version of the figure is available online at *QJMAM*)

found via the Cagniard–De Hoop technique (viz. (5.8)) as well as using the one obtained via the modal-expansion approach (viz. (5.11)). The second part of this section provides an example of the time-varying spatial distribution of the wavefield $u = u(x_1, x_3, t)$ in $\mathcal{D}$. The pulse time width of the excitation is chosen such that the separate reflected time-domain constituents can be clearly distinguished. As the excitation pulse we take the power exponential excitation signature:

$$F(t) = F_{\max}(t/t_r)^{\nu} \exp[-\nu(t/t_r - 1)]\mathrm{H}(t), \tag{6.1}$$

where $F_{\max}$ is the pulse amplitude, t_r is the pulse rise time and $\nu > 0$ is the rising exponent. The pulse time width t_w is then related to t_r and ν via

$$t_w = t_r\, \nu^{-\nu-1}\Gamma(\nu + 1)\exp(\nu), \tag{6.2}$$

where $\Gamma(x)$ is the Euler gamma function. In the following examples we take the power exponential source signature with the spatial support $ct_w/H = 0.5$, with the rising exponent $\nu = 2$ and amplitude $F_{\max} = 1$. The corresponding pulse rise time is $ct_r/H = 0.2707$ (Fig. 3). In all calculations we take $c = 1$. The horizontal offset of the source is $x_{1;S} = H$ and the spatial solution domain is $\mathcal{D} = \{0 \leqslant x_1 \leqslant 2H, 0 \leqslant x_3 \leqslant H\}$, that is $W = 2H$.

The pulse shape of fundamental solution u^F is observed at the point $(x_1, x_3) = (2H, 0.8H)$ within the time window $\{0 \leqslant ct/H \leqslant 10\}$. Figure 4 show the fundamental solution evaluated using the Cagniard–De Hoop method. Figure 4a clearly illustrates that each higher time-domain constituent arrives at the observation point at a later time than the previous one. For the chosen time window, only the first five time-domain constituents are sufficient to get results within any prescribed precision. In contrast to these results, Figs 5a show the particular modal constituents (first five) and the fundamental solution, respectively, found via the modal-expansion approach. It is clear that all modal constituents arrive at the same axial arrival time X_1/c and for practical calculations the sum in (5.11) must be always truncated. Since the oscillations of the modal constituents increase with the order of modes, a fine integration technique must be used to take into the account the high-order modes. In Fig. 5b is illustrated a typical shaky behaviour for an insuficient number (here $\Gamma = 5$) of the modal constituents included (symbol ∞ in (5.11) is replaced with Γ). In that case, the modal solution may provide

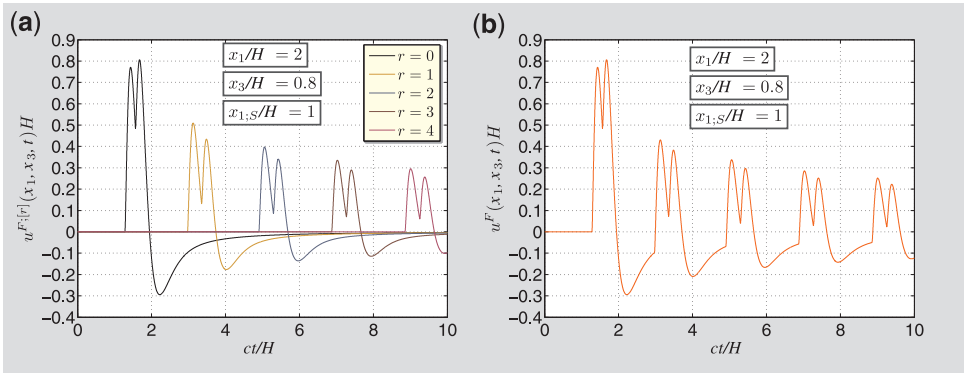

Fig. 4 (a) Particular time-domain constituents of the generalised-ray expansion; (b) Fundamental solution evaluated via the Cagniard–De Hoop method (Colour version of the figures are available online at *QJMAM*)

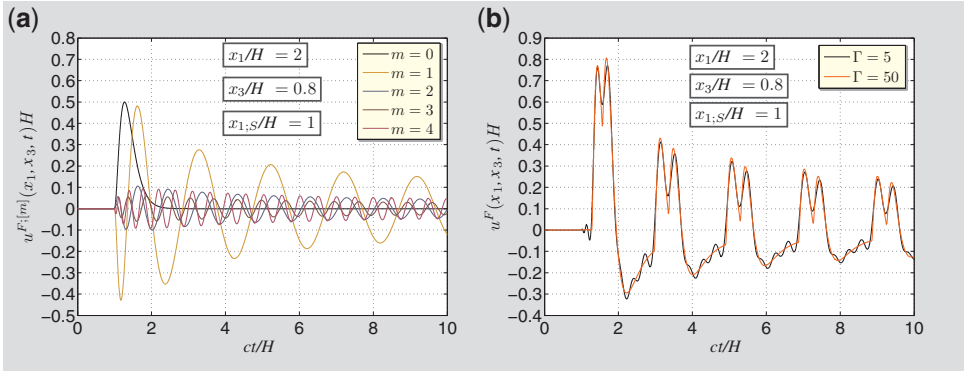

Fig. 5 (a) Particular time-domain constituents of the modal-expansion approach; (b) Fundamental solution evaluated via the modal-expansion method (Colour version of the figures are available online at *QJMAM*)

misleading information about the arrival time of the relevant wave motion. As can be seen, the trembling is canceled out for $\Gamma = 50$.

Next example demonstrates the time evolution of the spatial distribution of $u = u(x_1, x_3, t)$ given in (5.12). It is clear that up to $ct/H = 1.0$ the wave does not reach the boundaries and the solution (5.13) equals to the one for an open half-space in $\{0 \leqslant ct/H < 1.0\}$. To observe effects of boundaries we therefore choose the observation times $ct/H = \{1.5, 2.0\}$. Figure 6 show the spatial distribution of $u = u(x_1, x_3, t)$ that is closed by the Neumann-type boundaries, that is $\partial_1 u = 0$ along $x_1 = 0$ and $x_1 = 2H$ with (5.2) and (5.3), at two observation times $ct/H = \{1.5, 2.0\}$, respectively. Figure 6a shows the reflected wavefronts on a halfway back towards the activating line source. Figure 6b then illustrates a somewhat more complex wavefield distribution consisting of reflected waves from the horizontal as well as from the vertical boundaries.

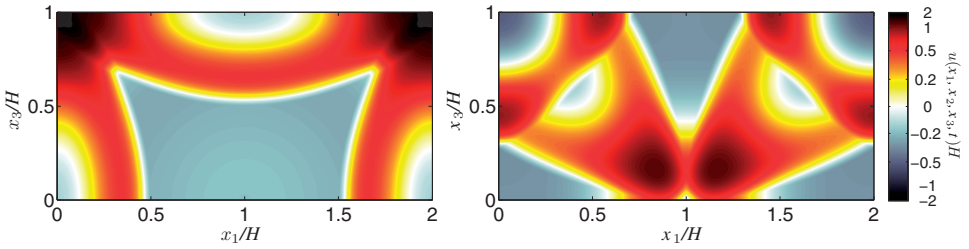

Fig. 6 Wave field distribution for boundary conditions: $\partial_1 u = 0$ along $x_1 = 0$ and $x_1 = 2H$ ($\partial_3 u = 0$ along $x_3 = 0$ exluding the source point and $x_3 = H$) at (a) $ct/H = 1.5$; (b) $ct/H = 2.0$ (Colour version of the figures are available online at *QJMAM*)

7. Conclusions

It has been demonstrated that the Cagniard–De Hoop technique is capable of handling a large class of initial-boundary value problems solved in bounded regions with plane boundaries. A general solution consists of a superposition of the time-domain constituents a subset of which represents an effect of additional boundaries. The presented procedure extends applications of the Cagniard–De Hoop technique in an analytical benchmarking of direct discretization numerical techniques that solve the field equations in bounded solution domains.

Acknowledgements

The research described in this article has received funding from the project CZ.1.07/2.3.00/30.0005 of the Brno University of Technology.

References

1. A. T. De Hoop, A modification of Cagniard's method for solving seismic pulse problems, *Appl. Sci. Res.* **B8** (1960) 349–356.
2. L. Cagniard, *Réflexion et réfraction des ondes sésimiques progressives* (Gauthier-Villars, Paris 1939).
3. L. Cagniard, *Reflection and Refraction of Progressive Seismic Waves* (Translation by E. Flinn and C. H. Dix of *Réflexion et réfraction des ondes sésimiques progressives*, Gauthier-Villars, Paris 1939) McGraw-Hill, New York 1962.
4. C. Chapman, *Fundamentals of Seismic Wave Propagation* (Cambridge University Press, Cambridge, UK 2004).
5. K. Aki and P. G. Richards, *Quantitative Seismology*, 2nd edn (Sausalito, University Science Books, CA 2009).
6. G. G. Drijkoningen and J. T. Fokkema, The exact seismic response of an ocean and a N-layer configuration, *Geophys. Pros.* **35** (1987) 33–61.
7. A. T. De Hoop and H. J. Frankena, Radiation of pulses generated by a vertical electric dipole above a plane, non-conducting, earth, *Appl. Sci. Res.* **B8** (1960) 369–377.
8. A. T. De Hoop, Pulsed electromagnetic radiation from a line source in a two-media configuration, *Radio Sci.* **14** (1979) 253–268.

9. A. T. De Hoop and M. L. Oristaglio, Application of the modified Cagniard technique to transient electromagnetic diffusion problems, *Geophys. J.* **94** (1988) 387–397.
10. A. T. De Hoop, Transient diffusive electromagnetic fields in stratified media – calculation of the two-dimensional E-polarized field, *Radio Sci.* **35** (2000) 443–453.
11. A. T. De Hoop, M. Štumpf, and I. E. Lager, Pulsed electromagnetic field radiation from a wide slot antenna with a dielectric layer, *IEEE Trans. Antennas Propag.* **59** (2011) 2789–2798.
12. A. T. De Hoop and J. H. M. T. van der Hijden, Generation of acoustic waves by an impulsive line source in a fluid/solid configuration with a plane boundary, *J. Acoust. Soc. Am.* **74** (1983) 333–342.
13. A. T. De Hoop and J. H. M. T. van der Hijden, Generation of acoustic waves by an impulsive point source in a fluid/solid configuration with a plane boundary, *J. Acoust. Soc. Am.* **75** (1984) 1709–1715.
14. J. D. Achenbach, *Wave Propagation in Elastic Solids* (Amsterdam, North-Holland, the Netherlands 1976).
15. A. T. De Hoop and J. H. M. T. van der Hijden, Seismic waves generated by an impulsive point source in a solid/fluid configuration with a plane boundary, *Geophysics* **50** (1985) 1083–1090.
16. J. H. M. T. van der Hijden, *Propagation of Transient Elastic Waves in Stratified Anisotropic Media* (Amsterdam, North-Holland, the Netherlands 1987).
17. A. T. De Hoop, Acoustic radiation from impulsive sources in a layered fluid, *Nieuw Archief voor Wiskunde*, ser. **4** (1988) 111–129.
18. A. T. De Hoop, Acoustic radiation from an impulsive point source in a continuously layered fluid – an analysis based on the Cagniard method, *J. Acoust. Soc. Am.* **88** (1990) 2376–2388.
19. M. D. Verweij, Transient acoustic wave modeling: higher-order Wentzel-Kramers-Brillouin-Jeffreys asymptotics and symbolic manipulation, *J. Acoust. Soc. Am.* **92** (1992) 2223–2238.
20. C. H. Chapman, Exact and approximate generalized ray theory in vertically inhomogeneous media, *Geophys. J. Roy. Astr. Soc.* **46** (1976) 201–233.
21. E. Zauderer, *Partial Differential Equations of Applied Mathematics*, 2nd edn (New York, John Wiley & Sons, NY 1989).
22. I. E. Lager and A. T. De Hoop, Time-domain receiving properties of a multimode cylindrical waveguide antenna, *Proc. 5th EUropean Conference on Antennas and Propagation* (Rome, Italy, April 2011), 1341–1344.
23. A. T. De Hoop, *Handbook of Radiation and Scattering of Waves* (Academic Press, London, UK 1995).
24. P. M. Morse and H. Feshbach, *Methods of Theoretical Physics*, Part I (New York, McGraw-Hill Book Company, Inc., NY 1953).
25. G. Doetsch, *Introduction to the Theory and Application of the Laplace transformation* (Springer-Verlag, Berlin, Germany 1974).
26. G. G. Drijkoningen and C. H. Chapman, Tunneling ray using the Cagniard-De Hoop method, *B. Seismol. Soc. Am.* **78** (1988) 898–907.
27. M. Abramowitz and I. A. Stegun, *Handbook of Mathematical Functions*, 10th printing (with corrections) (New York, Dover Publications, NY 1972).